Macromolecules

Volume 16, Number 3 March 1983

Isotactic Polymerization of 3-Methyl-1-pentene: Enantioselectivity and Diastereoselectivity

Adolfo Zambelli* and Paolo Ammendola

Istituto Chimico, Università di Napoli, 80134 Napoli, Italy

Maria Carmela Sacchi, Paolo Locatelli, and Giulio Zannoni

Istituto di Chimica delle Macromolecole, CNR, 20133 Milano, Italy.
Received August 3, 1982

ABSTRACT: The stereochemical structures of isotactic polymers of (*S*)- and (*RS*)-3-methyl-1-pentene, selectively enriched in ^{13}C, have been investigated by ^{13}C NMR. The stereoselectivity of the polymerization has been quantitatively evaluated. It is suggested that stereoselectivity arises from the higher reactivity of the *R',R* and *S',S* monomer faces in comparison with the *R',S* and *S',R* faces and from the mechanism of the enantioselective control.

1. Introduction

As discovered by Natta and co-workers, isotactic poly[(*RS*)-3-methyl-1-pentene] consists of enantiomeric macromolecules and can be resolved, at least partially, by liquid chromatography on an appropriate optically active support.[1,2]

In order to account for this fact it has been suggested that the Ziegler–Natta isotactic-specific polymerization catalyst is a racemic mixture of asymmetric active sites, which, depending on the configuration, react preferentially with either one or the other antipode of (*RS*)-3-methyl-1-pentene [(*RS*)-3MP1].[1-4]

Stereochemical investigation of isotactic polypropylene showed that isotactic propagation arises from the enantioselectivity[5,6] of the incorporation of the prochiral monomer on the reactive metal–alkyl bonds of chiral active sites.

In addition to the chirality of the active site, the occurrence of enantioselective incorporation requires that the alkyl group bonded to the active metal must be larger than CH_3.[7] As a consequence of the mechanism of the enantioselective propagation, the stereochemical sequence of the configurations of isotactic poly(α-olefins) obtained in the presence of Ziegler–Natta catalysts is typically ... mmmmrrmmm...mmrrmmm,[5,8,9] i.e., sequences of m dyads connected by pairs of r dyads (see Figure 1a). It seems reasonable that the stereochemical sequence of the configurations of the substituted carbons of the backbone should be basically the same for isotactic poly(3MP1) and isotactic polypropylene. On the other hand, the faces of 3MP1 are diastereotopic and the insertion reaction should be more or less diastereoselective (Figure 2).

The quoted results[1,2] concerning polymerization of (*RS*)-3MP1 could arise, in agreement with the hypothesis of Natta and co-workers,[1] from the enantioselectivity of the chiral active sites toward the enantiotopic carbon of the monomer and from the diastereoselectivity of the incorporation of 3MP1.[3]

This paper deals with the determination of the stereochemical structure of both isotactic poly[(*RS*)-3MP1] and poly[(*S*)-3MP1] and the information concerning the reaction mechanism that can be derived. The stereochemical structure of the end groups is a particular focus of attention.

2. Results and Discussion

Poly[(*RS*)-3MP1]. In Figure 3A is shown the ^{13}C NMR spectrum of the fraction of poly[(*RS*)-3MP1] soluble in boiling benzene. The polymer was prepared in the presence of δ-$TiCl_3$/$Al(^{13}CH_3)_3$/$Zn(^{13}CH_3)_2$. The resonances at 13.2_4, 13.4_3, 15.0_9, and 15.2_7 ppm from hexamethyldisiloxane (HMDS) are due to the enriched carbon of 2,3-dimethyl-(2'-^{13}C)pentyl end groups in different stereochemical environments. Such end groups come from the incorporation of the first monomer unit on the metal–(^{13}C)methyl (Mt–$^{13}CH_3$) bonds of the active sites (initiation).

$$Mt\text{–}^{13}CH_3 \rightarrow Mt\text{–}(CH_2CH(sec\text{-}C_4H_9))^{13}CH_3$$

Hereafter they will be called "right" end groups since the Mt of the active sites is arbitrarily assumed to be on the left side of the growing polymer chain.

The assignment of the above chemical shifts is achieved on the basis of the additivity rule of Grant and Paul[10] and

0024-9297/83/2216-0341$01.50/0

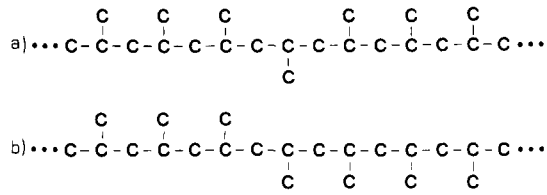

Figure 1. The structure of the isotactic chain is shown in (a). The structure reported in b, nearly absent in highly isotactic polypropylene, would involve a different mechanism of steric control, as suggested by Shelden et al.[6]

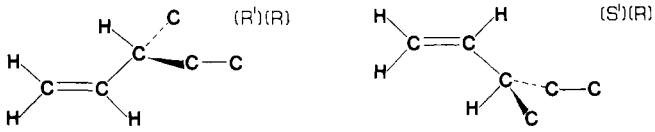

Figure 2. The faces of chiral α-olefins are diastereotopic. In the figure are reported the diastereotopic faces of (*R*)-3-methyl-1-pentene. In order to distinguish the diastereotopic faces, we use in this paper the absolute[10] configuration of carbon 3 and the absolute configuration assumed by carbon 2 when the observed face is coordinated to a transition-metal atom. This latter configuration is primed to avoid any possible confusion. Of course, the faces of the *S* monomer are mirror images of the reported ones.

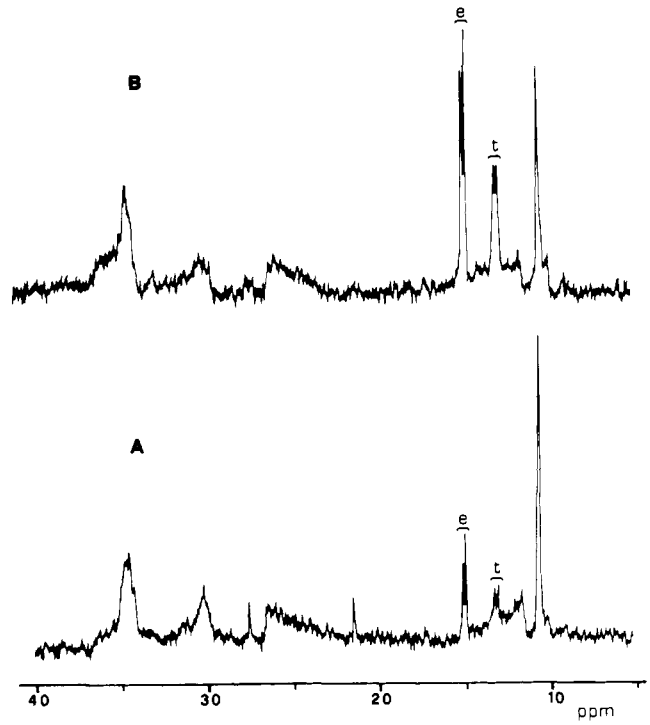

Figure 3. ^{13}C NMR spectra of (A) benzene-soluble fraction of poly[(*RS*)-3MP1] and (B) acetone-soluble fraction of the same sample (for the explanation, see text) (HMDS scale).

from the fact that these resonances are not observed in the spectrum of a similar fraction prepared without ^{13}C-enriched organometallic cocatalysts.

In Figure 4 are shown the eight diastereomer stereochemical environments of ^{13}C-enriched carbons that can result from the incorporation of two monomer units, considering both the backbone and the side-chain asymmetric carbons.[12] A nearly complete assignment of the observed resonances is reported in the following sections.

What is relevant here is that the resonances at 15.0_9 and 15.2_7 ppm are due to enriched methyls having an erythro steric relationship with an additional vicinal methyl substituent (Figure 4A) and that the resonances at 13.2_4 and 13.4_3 ppm are due to enriched methyls having a threo steric relationship with an additional vicinal methyl substituent

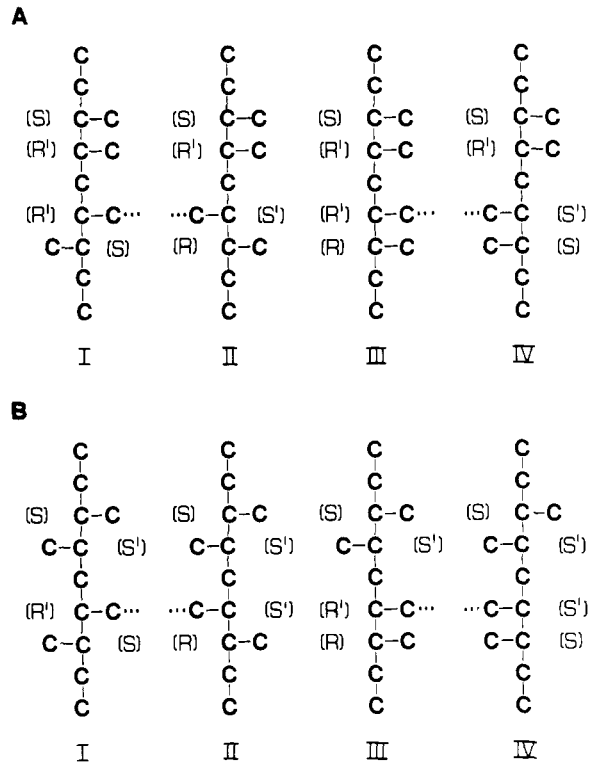

Figure 4. Fischer projections of the possible stereochemical environments of the ^{13}C of the 2,3-dimethyl-(2′-^{13}C)pentyl end groups. The configurational relationship with the further substituted carbons is considered up to a distance of five bonds. The configuration of the ^{13}C substituted carbon is attributed on the basis of ref 11, but neglecting the isotopic substitution; i.e., the $^{13}CH_3$ substituent is considered as the one having the lower rank (see caption of Figure 5 and note 12).

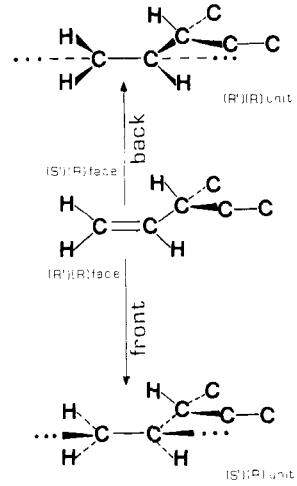

Figure 5. Diastereomeric monomer units arise from incorporation of 3MP1 on the growing polymer chain, depending on the reacting diastereotopic monomer face. In the figure is shown the monomer unit arising from the attack on the front face (down) and the back face (up) of (*R*)-3-methyl-1-pentene. For the assignment of the configuration of the backbone substituted carbon of the monomer unit it is considered that the left side of the chain has a higher rank than the right one since, by definition, it is also assumed that the metal atom of the active site is at the left side of the polymer chain. Note that according to this definition, attack on *R*′ (or *S*′) faces gives *S*′ (or *R*′) carbons on the backbone.

(Figure 4B).[13] This last assignment can be simply reached by comparing the observed chemical shifts with those reported in the literature[14] for C_6' and C_7' of *meso*- and *rac*-6,7-dimethyldodecane.

Table I
Fractionation Results and Diastereoselectivity Data for Poly[(*RS*)-3MP1]

fraction	wt %	e/t[a]	$(\overline{MW})_n$[b]
acetone soluble	12	$1._9$	1_{000}
acetone insoluble, diethyl ether soluble	4.6	$2._0$	2_{000}
diethyl ether insoluble, benzene soluble	3.3	$1._8$	2_{800}
benzene insoluble, toluene soluble	2.4	$2._0$	3_{100}
toluene insoluble[c]	77.7	$2._1$	12_{000}

[a] e/t represents the intensity ratio between the resonances of the ^{13}C-enriched methyl carbons in erythro (15.0_9 and 15.2_7 ppm) and threo (respectively, 13.2_4 and 13.4_3 ppm) configurational relationship with respect to the further vicinal methyl substituent. See also text and ref 13. [b] $\overline{MW}_n$'s have been estimated assuming the presence of one $^{13}CH_3$ per chain, from the intensity ratio between the resonances of the enriched CH_3's of the end groups and the resonance of C_5. They may be affected by systematic error because the possible difference of T_1's has not been carefully considered. [c] The toluene-insoluble fraction was examined after thermal degradation. Epimerization of the end groups should be negligible (see footnote *c* of Table II).

The erythro arrangement arises from an attack on the face of the monomer having the same configuration as the asymmetric carbon of the substituent, while the threo arrangement comes from an attack on the other diastereotopic face (see Figure 5). The relative intensities of the erythro and the threo $^{13}CH_3$ resonances ($\sim$2/1) (see Figure 3) show that insertion on the metal–methyl bond of the active site is moderately diastereoselective and that the faces of the monomer having the same configuration (see Figure 5) as the chiral carbon of the substituent are the more reactive ones.

It may be worthwhile to observe that the more reactive diastereotopic faces in the insertion are those giving less thermodynamically stable complexes in solution with both square-planar[15,16] and trigonal-bipyramidal Pt.[17] It should be further noted that the fraction of polymer under consideration is crystalline by X-ray analysis (see Figure 7) and that the solubility is to be attributed to low molecular weight. The molecular weight can be roughly estimated from the intensity ratio between the resonances of the ^{13}C-enriched carbons of the end groups and, for example, the resonances of carbon 5 of the inner monomer units (see Table I). The carbons are labeled in the inner monomer units in the same manner as in the monomer, i.e.

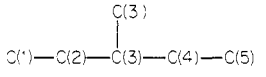

Hence, this fraction is representative of the highly isotactic part of the polymer.

As previously mentioned,[7] the insertion of α-olefins into $Mt–CH_3$ bonds is not enantioselective with regard to the enantiotopic carbon of the monomer. In addition, nearly equal intensity ratios have been observed for these resonances in all the polymer fractions, including the more soluble ones (see Table I and Figure 3B). This seems to indicate that the enantioselectivity and the diastereoselectivity of the insertion are independent, although both are needed for the occurrence of "stereoselective"[1,2] polymerization.

Two additional sharp resonance peaks are observed at 21.5_8 and 27.6_3 ppm in Figure 3A. On the basis of the additivity rule of Grant and Paul[10] they appear to arise from a few ^{13}C-enriched ethylene comonomer units. The origin of these units will be considered in a future paper.

Table II
Fractionation Results and Diastereoselectivity Data for Poly[(*S*)-3MP1]

fraction	wt %	e/t[a]	$(\overline{MW})_n$[b]
acetone soluble	15.4	$1._7$	1_{600}
acetone insoluble, diethyl ether soluble	19.2	$1._8$	3_{100}
diethyl ether insoluble, benzene soluble	9.4	$1._7$	4_{400}
benzene insoluble, toluene soluble	7.4	$1._9$	4_{700}
toluene insoluble[c]	48.6	$2._0$	8_{400}

[a] e/t represents the intensity ratio between the resonances of the ^{13}C-enriched methyl carbons in erythro (15.0_9 ppm) and threo (respectively, 13.4_5 and 13.5_7 ppm) configurational relationships with respect to the vicinal methyl substituent (see also ref 13). [b] See footnote *b* of Table I. [c] The toluene-insoluble fraction was examined after thermal degradation. The resonances of the carbons of the inner monomer units were marginally affected by epimerization. Therefore it is reasonable that epimerization of the end groups is nearly negligible.

Table III
^{13}C Chemical Shifts[a] Observed in Poly[(*S*)-3MP1] for the Inner Monomer Units

carbon[b]	ν[c]	carbon[b]	ν[c]
1	30.3_3	3′	11.8_0
2 or 3	34.3_6	4	26.6_5
3 or 2	34.6_7	5	10.7_9

[a] Measured from internal HMDS. [b] See the drawing in Figure 1. [c] The assignment of the observed resonances was made on the basis of the Grant and Paul rule.[10]

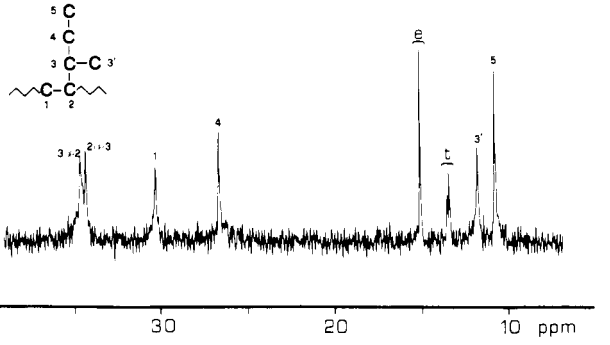

Figure 6. ^{13}C NMR spectrum of benzene-soluble fraction of poly[(S)-3MP1] (HMDS scale).

Poly[(*S*)-3MP1]. For deeper insight into the problem we prepared a sample of isotactic poly[(*S*)-3MP1] in the presence of the previously mentioned ^{13}C-enriched catalyst system and under the same conditions used for (*RS*)-3MP1. The polymer was fractionated with boiling solvents as reported in Table II, and the fractions were analyzed by ^{13}C NMR. The spectrum of the fraction soluble in boiling benzene and insoluble in boiling diethyl ether[18] is shown in Figure 6. It looks remarkably different from that of the corresponding fraction of poly[(*RS*)-3MP1]. The resonances of the carbons of the inner monomer units (the assignments are reported in Table III) are very sharp, unlike those of poly[(*RS*)-3MP1]. The broadness of the resonances of poly[(*RS*)-3MP1] may be reasonably ascribed to stereochemical shifts arising from substituted carbons of different configurations. These carbons should not be those of the backbone since both polymers are highly crystalline. In Figure 7 are shown the X-ray spectra of both polymers; they indicate a highly isotactic structure.[19,20] The observed facts can be reconciled with the

Scheme I [a]

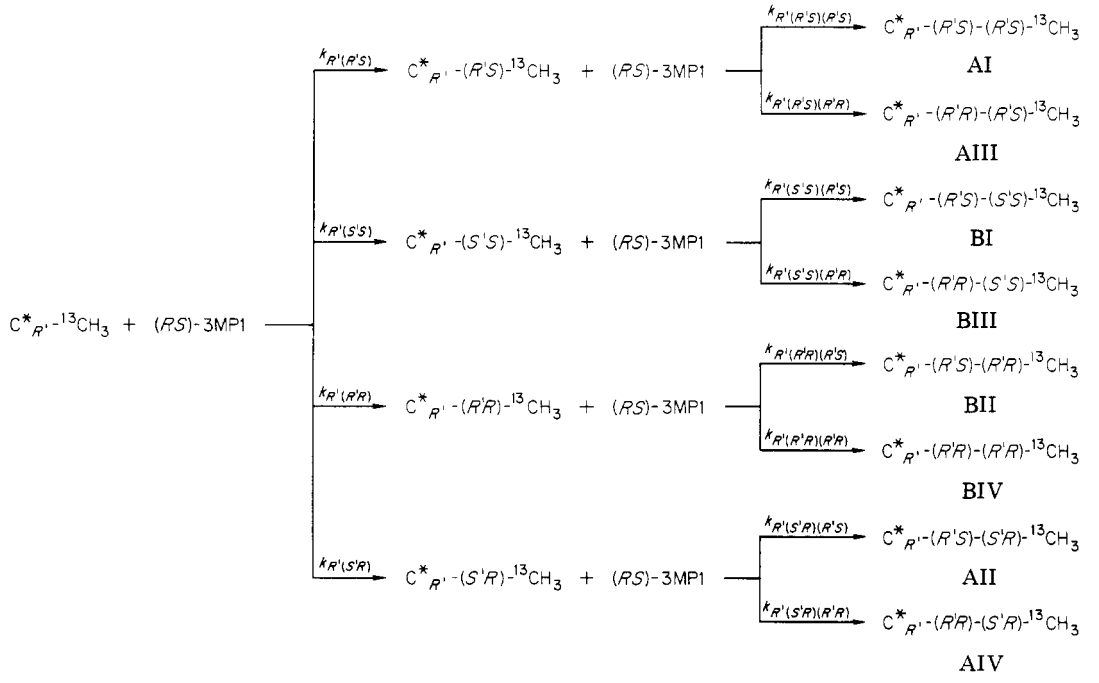

[a] Reference 21.

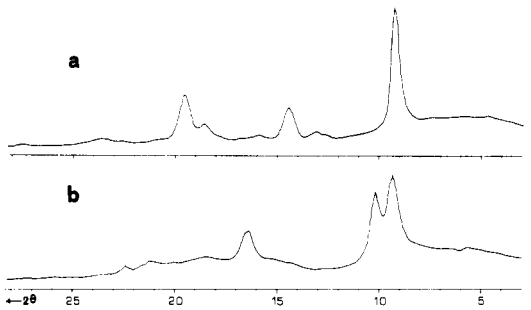

Figure 7. Geiger counter registered X-ray diffraction powder spectra (Cu Kα radiation) of (a) benzene-soluble fraction of poly[(*S*)-3MP1] and (b) benzene-soluble fraction of poly[(*RS*)-3MP1].

results of Natta and Pino[1,2] assuming that poly[(*RS*)-3MP1] consists of enantiomorphic macromolecules not quite optically pure and with a Bernoullian stereochemical sequence of the configurations of the chiral substituents. This assumes some isomorphism between the *R* and *S* substituents of the polymer chain. The resonances at 15.0_9, 13.4_5, and 13.5_7 ppm in the spectrum of Figure 6 are again due to $^{13}CH_3$ of the "right" end groups arising from the initiation step. As reported above, the resonance at 15.0_9 ppm is due to $^{13}CH_3$ in an erythro relationship with an additional vicinal methyl of the first monomer unit of the chain, and the resonances at 13.4_5 and 13.5_7 ppm are due to $^{13}CH_3$ in a threo relationship. From the intensity ratio between these resonances it may be seen that the erythro $^{13}CH_3$/threo $^{13}CH_3$ (e/t) ratio is essentially the same as in poly[(*RS*)-3MP1] (compare Tables I and II). The same observation can be made by considering the other polymer fractions reported in the tables. The higher reactivity of the *S'*,*S* face of the monomer is thus confirmed. However, only three resonances are observed for the $^{13}CH_3$ of poly[(*S*)-3MP1] and the chemical shifts do not coincide entirely with those observed for poly[(*RS*)-3MP1]. This is not surprising when one considers the influence of the stereochemical structure of the second neighboring unit on the chemical shift. The possible stereochemical environments of $^{13}CH_3$ in poly[(*RS*)-3MP1] are those reported in

Table IV
Molar Fractions Calculated for the Different Stereochemical Environments of the ^{13}C-Enriched Methyl Carbons of the "Right" End Groups under the Hypotheses Given in the Text

stereochemical environment[a]	molar fraction (calcd) poly[(*RS*)-3MP1]	poly[(*S*)-3MP1]
AI	0.22	0.33
AII	0.22	
AIII	0.11	
AIV	0.11	0.33
BI	0.11	0.17
BII	0.11	
BIII	0.06	
BIV	0.06	0.17

[a] The corresponding drawing of the chain end groups in Fisher projection are reported in Figure 4.

Scheme I, where it is assumed that (1) the insertion of the first monomer unit (into $Mt-^{13}CH_3$ bonds) is not enantioselective,[7] (2) the insertion of the next unit is highly enantioselective according to the chirality of the active site,[5,7] and (3) the insertion of all the units is only partially diastereoselective. According to Scheme I the diastereoselectivity of the initiation on the $C^*_{R'}$ is

$$\frac{e}{t} = \frac{I_A}{I_B} = \frac{k_{R'(R'S)} + k_{R'(S'R)}}{k_{R'(S'S)} + k_{R'(R'R)}} \quad (1)$$

where I_A and I_B are the intensities of the $^{13}CH_3$ resonances of the A and B "right" end groups shown in Figure 4. A mirror equation applies to the *S'*-preferring sites ($C^*_{S'}$). Assuming that the diastereoselectivity is the same for all the steps, the relative concentration of the end groups should be as shown in Table IV on the basis of the experimentally determined e/t ratios. The possible stereochemical environments of $^{13}CH_3$ in poly[(*S*)-3MP1] are shown in Scheme II. It should be observed that Scheme II involves the same assumptions as Scheme I. Both $C^*_{S'}$ and $C^*_{R'}$ are considered since, due to the presence of only (*S*)-3MP1, the steps occurring on enantiomorphic sites are no longer in a mirror relationship. The "right" end groups

Scheme II[a]

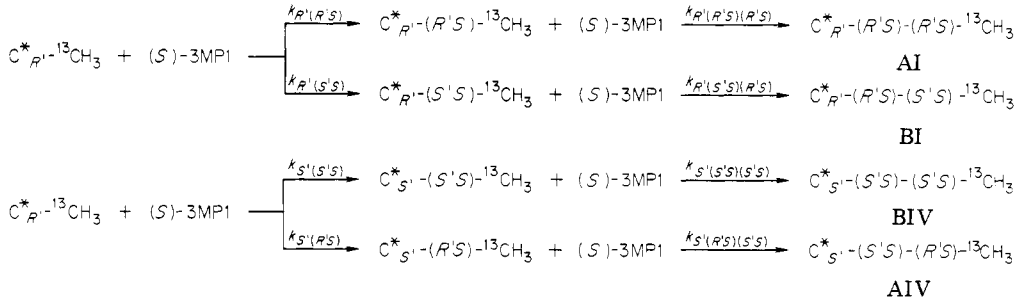

[a] Reference 21.

considered here come from insertion on active sites bearing ^{13}C-enriched methyl group. The proportion of the different end groups is proportional to the rate of the four initiation steps of Scheme II so that

$$\frac{e}{t} = \frac{I_{AI} + I_{AIV}}{I_{BI} + I_{BIV}} = \frac{k_{R'(R'S)}[C^*_{R'}\text{–}^{13}CH_3] + k_{S'(R'S)}[C^*_{S'}\text{–}^{13}CH_3]}{k_{R'(S'S)}[C^*_{R'}\text{–}^{13}CH_3] + k_{S'(S'S)}[C^*_{S'}\text{–}^{13}CH_3]} \quad (2)$$

Due to the presence of fast chain transfer with $Zn(^{13}CH_3)_2$[19] $C^*\text{–}^{13}CH_3$ sites are continuously formed and disappear after the initiation:

$$C^*\text{–}(CH_2CH(sec\text{-}C_4H_9))_n\text{–}^{13}CH_3 + Zn(^{13}CH_3)_2 \rightarrow C^*\text{–}^{13}CH_3 + Zn(^{13}CH_3)\text{–}(CH_2CH(sec\text{-}C_4H_9))_n\text{–}^{13}CH_3$$

Under steady-state conditions

$$k_{Zn(R')}[C^*_{R'}\text{–}(CH_2CH(sec\text{-}C_4H_9))_n\text{–}^{13}CH_3][Zn(^{13}CH_3)_2] = (k_{R'(R'S)} + k_{R'(S'S)})[C^*_{R'}\text{–}^{13}CH_3][(S)\text{-3MP1}] \quad (3)$$

i.e.

$$[C^*_{R'}\text{–}^{13}CH_3] = \frac{k_{Zn(R')}[C^*_{R'}\text{–}(CH_2CH(sec\text{-}C_4H_9))_n\text{–}^{13}CH_3][Zn(^{13}CH_3)_2]}{(k_{R'(R'S)} + k_{R'(S'S)})[(S)\text{-3MP1}]} \quad (4)$$

where $k_{Zn(R')}$ is the rate constant of the chain transfer of $Zn(^{13}CH_3)_2$ with $C^*_{R'}\text{–}(CH_2CH(sec\text{-}C_4H_9))_n\text{–}^{13}CH_3$ (i.e., the chains growing on the R' sites). Of course, for the $C^*_{S'}$ sites

$$[C^*_{S'}\text{–}^{13}CH_3] = \frac{k_{Zn(S')}[C^*_{S'}\text{–}(CH_2CH(sec\text{-}C_4H_9))_n\text{–}^{13}CH_3][Zn(^{13}CH_3)_2]}{(k_{S'(R'S)} + k_{S'(S'S)})[(S)\text{-3MP1}]} \quad (5)$$

Assuming that the number of $C^*\text{–}^{13}CH_3$ (R' or S' preferring) sites is negligible in comparison with $C^*\text{–}(CH_2CH\text{-}(sec\text{-}C_4H_9))_n\text{–}^{13}CH_3$ and that the total amount of $C^*_{R'}$, bearing either a methyl or a growing chain, present on the surface of the catalyst is the same as that of $C^*_{S'}$, we may combine eq 4 and 5 with eq 2 to obtain the relation

$$\frac{e}{t} = \frac{I_{AI} + I_{AIV}}{I_{BI} + I_{BIV}} = [k_{Zn(R')}k_{R'(R'S)}(k_{S'(S'S)} + k_{S'(R'S)}) + k_{Zn(S')}k_{S'(R'S)}(k_{R'(R'S)} + k_{R'(S'S)})]/[k_{Zn(R')}k_{R'(S'S)}(k_{S'(S'S)} + k_{S'(R'S)}) + k_{Zn(S')}k_{S'(S'S)}(k_{R'(R'S)} + k_{R'(S'S)})] \quad (6)$$

If the polymer fractions formed on $C^*_{R'}$ and $C^*_{S'}$ are considered separately one can derive

$$(e/t)_{C^*_{R'}} = I_{AI}/I_{BI} = k_{R'(R'S)}/k_{R'(S'S)} \quad (7)$$

and

$$(e/t)_{C^*_{S'}} = I_{AIV}/I_{BIV} = k_{S'(R'S)}/k_{S'(S'S)} \quad (8)$$

Table V
Chemical Shifts[a] of the ^{13}C-Enriched Methyl Carbons of the "Right" End Groups in Threo (t) and Erythro (e) Configurational Relationship

poly[(*RS*)-3MP1]			poly[(*S*)-3MP1]			end groups
t	e	I^b	t	e	I^b	
13.2_4		0.17				BII
13.4_3		0.18	13.4_5		0.22	BI
			13.5_7		0.14	BIV
	15.0_9	0.34		15.0_9	0.64	AI + AIV
	15.2_7	0.31				AII + AIII

[a] Measured from internal HMDS. [b] Approximate relative intensities on the benzene-soluble fractions.

In principle, it should be possible to separate the two fractions, for example, on the basis of differing molecular weights, since the propagation rate constants[22] should be different. It should thus be possible to evaluate separately the diastereoselectivity of the initiation of the S monomer on enantiomorphic sites. The efficiency of the separation can be evaluated from the stereochemical structure of the end groups. The end groups of the macromolecules formed on $C^*_{R'}$ should be AI and BI, while they should be AIV and BIV on the macromolecules grown on $C^*_{S'}$. As reported in the following (see Table V) the chemical shifts of the AI and AIV $^{13}CH_3$'s coincide, but those of BI and BIV are reasonably well resolved (see Figure 6). The ratio between the intensities of these resonances (I_{BI}/I_{BIV}) increases roughly from 1.1 up to 2.2 going from the ether-soluble to the toluene-soluble fraction. This shows that fractionation with solvents of different boiling point is at least partially successful.[23] Assuming that the chain-transfer reaction is not diastereoselective, the increase of the I_{BI}/I_{BIV} ratio with increasing molecular weight (Table II) suggests that for (*S*)-3MP1, chain propagation is faster on $C^*_{R'}$ than on $C^*_{S'}$ sites. However, the most important observation is that the same overall e/t ratio [$=(I_{AI} + I_{AIV})/(I_{BI} + I_{BIV})$] is found in all the fractions of Table II and is practically the same as observed for poly[(*RS*)-3MP1] (see Table I). One can conclude that $k_{R'(R'S)}/k_{R'(S'S)} = k_{S'(R'S)}/k_{S'(S'S)}$, i.e., the diastereoselectivity, is independent of the relative configuration of the active site and the substituent of the reacting monomer.

A nearly complete assignment of the chemical shift of the $^{13}CH_3$ as a function of the stereochemical structure of the end groups, reported in Figure 4, can be achieved by comparing the calculated molar fractions of the different end groups of isotactic poly[(*RS*)-3MP1] and poly[(*S*)-3MP1] (Table IV) with the intensities and chemical shifts observed for the $^{13}CH_3$ in the polymers under consideration (Table V). Under the assumptions of Schemes I and II, only AI, AIV, BI, and BIV end groups are present in poly[(*S*)-3MP1]. Since only one resonance is detected in the erythro $^{13}CH_3$ region in Figure 1, at 15.0_9 ppm, the

chemical shifts of AI and AIV should coincide. The resonance observed at 15.2_7 ppm in the spectrum of poly[(*RS*)-3MP1] should account for the $^{13}CH_3$ of AII and AIII. The resonance at 13.2_4 ppm, observed only in the spectrum of poly[(*RS*)-3MP1], should be assigned to BII because this end group can occur only in this polymer. The resonance at 13.4_5 ppm, common to both polymers, has to be assigned to BI. The BIII $^{13}CH_3$ resonance is lost because of its low concentration in both polymers. The resonance at 13.5_7 ppm should be assigned to BIV since it is detected only in poly[(*S*)-3MP1]. Probably BIV is lost in the spectrum of poly[(*RS*)-3MP1], in agreement with the expected low concentration. The assignments are summarized in Table V.

Poly[(*RS*)-(1-^{13}C)3MP1]. It is shown in the above discussion that the *R',R* and *S',S* faces of 3MP1, i.e., those having the same absolute configuration as the asymmetric carbon of the substituent, are twice as reactive as the *R',S* and *S',R* faces toward the insertion on the active Mt–CH_3 bonds (initiation step) of the Ziegler–Natta isotactic catalytic system δ-$TiCl_3$/$Al(CH_3)_3$/$Zn(CH_3)_2$. However, the initiation step is not enantioselective toward the enantiotopic carbon of the monomer[7] and is followed by a number of insertion steps on Mt–$(C_6H_{12})_n$–CH_3 bonds (chain propagation steps) that are highly enantioselective according to the chirality of the active sites.[5-7] Assuming that the propagation steps are as diastereoselective as the initiation step and bearing in mind the model of isotactic propagation, one may understand how it comes about that isotactic poly[(*RS*)-3MP1] consists of enantiomorphic macromolecules, as discovered by Natta and co-workers[1] (stereoselective polymerization). The whole polymer should be a mixture of two copolymers containing the *R* and *S* monomers in roughly 2/1 and 1/2 ratios, respectively, with a Bernoullian distribution. Actually, the broadness of the ^{13}C resonances found for poly[(*RS*)-3MP1], in comparison with the sharp resonances found for poly[(*S*)-3MP1], suggests a moderate optical purity of the enantiomorphic chains and a Bernoullian stereochemical sequence of the configurations of the substituents. However, direct information on the matter could be achieved only by observing the actual diastereoselectivity of the insertion during the propagation steps. The monomer units are diastereomeric and the configurational relationship between the reacting faces and the resulting monomer units is the following:

attacked face	resulting monomer unit	
R',R	...(*S',R*)...	(a)
S',S	...(*R',S*)...	(a')
R',S	...(*S',S*)...	(b)
S',R	...(*R',R*)...	(b')

Therefore, diastereoselectivity of the propagation could be evaluated by determining whether macromolecules consist mainly of a (a') or of b (b') units. However, symmetry considerations show that macromolecules of infinite length ...aaa... and ...b'b'b'... as well as ...a'a'a'... and ...bbb... are degenerate. Of course, isotactic copolymer macromolecules, e.g., ...aabab..., are not degenerate with the above homopolymers but such a copolymer block is degenerate with ...b'b'a'b'a'... . As a consequence, if the end groups are neglected, one can appreciate to what extent the reactivity of the diastereotopic faces is different, but one cannot say which are the more reactive ones. In this discussion we have tried to evade this difficulty by considering the stereochemical structure of the "left" end groups of isotactic poly[(*RS*)-(1-^{13}C)3MP1]. In Figure 8 is shown the ^{13}C NMR spectrum of the fraction soluble in boiling toluene and insoluble in boiling acetone of poly-

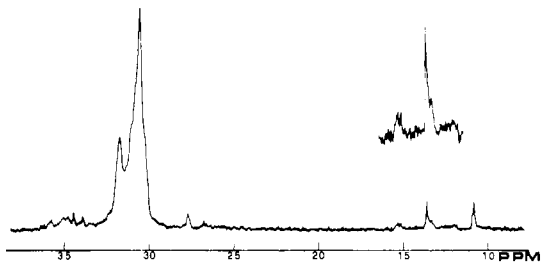

Figure 8. ^{13}C NMR spectrum of the fraction of poly[(*RS*)-(1-^{13}C)3MP1] soluble in boiling toluene and insoluble in boiling acetone (HMDS scale).

[(*RS*)-(1-^{13}C)3MP1], prepared in the presence of δ-$TiCl_3$/$Al(CH_3)_3$/$Zn(CH_3)_2$. Since the monomer instead of the cocatalysts is ^{13}C enriched, the $^{13}CH_3$ resonances (13.2_8, 13.5_9, 15.1_0, and 15.2_7 ppm from HMDS) arise from hydrolysis of the metal–methylene bonds involving either the metal of the active sites or Zn after the chain-transfer reaction:[24]

$$\text{Mt–}^{13}\text{CH}_2\text{CH}(sec\text{-}C_4H_9)\text{...} + \text{Zn}(CH_3)_2 \rightarrow$$
$$\text{Mt–CH}_3 + \text{Zn}(CH_3)\text{–}^{13}\text{CH}_2\text{CH}(sec\text{-}C_4H_9)\text{...} \xrightarrow{H_2O}$$
$$\text{Zn(OH)}_2 + CH_4 + {}^{13}CH_3\text{–CH}(sec\text{-}C_4H_9)\text{...}$$

The $^{13}CH_3$ resonances at 15.1_0 and 15.2_7 ppm are erythro and those at 13.2_8 and 13.5_9 ppm are threo according to the assignment presented in the previous sections. In conformity with a previous paper,[24] these end groups will be called "left" in order to avoid any confusion with those previously considered ("right"), arising from the initiation step.

By considering a single monomer unit after insertion into a Mt–CH_3 bond

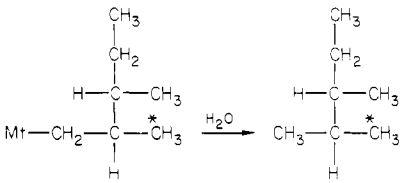

one can observe that because of the presence of the chiral carbon on the substituent, the positions of the Mt–CH_2 group and the starred CH_3 (the one bonded to Mt before the insertion) are diastereotopic.

Consequently, the starred methyl ("right") and that arising after hydrolysis of the metal–carbon bond ("left") will have different chemical shifts. The same occurs for the methyls of the "left" and the "right" end groups when they are spanned by several units of the same configuration instead of only one. Therefore the fact that the *e/t* ratio (i.e., the ratio of the intensities of the resonances of the erythro and the threo $^{13}CH_3$ of the left end groups) in Figure 8 is reversed in comparison with that observed for the "right" end groups means that in both cases the *R',R* and *S',S* faces of the monomer react faster.

If it is assumed that during polymerization chain transfer with the organometallic cocatalyst is not appreciably diastereoselective and that the propagation steps are highly enantioselective toward the enantiotopic carbon of the monomer,[5,7-9] it can be easily shown that the ratio of the intensities of the resonances of the $^{13}CH_3$'s of the left end groups is[25]

$$\frac{t}{e} = \frac{k_{R'(R'S)(R'S)} + k_{R'(R'R)(R'S)}}{k_{R'(R'S)(R'R)} + k_{R'(R'R)(R'R)}}$$

where the *k*'s are the kinetic constants for chain propagation steps, as defined in Scheme I.

Table VI
Assignment of the $^{13}CH_3$ of the "Left" End Groups

obsd $^{13}CH_3$ on the "left" end groups	ν, ppm	chemically equiv $^{13}CH_3$ on the "right" end groups	ν, ppm
$^{13}CH_3(R'S)(R'S)$...	13.5_9	...$(R'R)(R'R)^{13}CH_3$	13.5_7
$^{13}CH_3(R'S)(R'R)$...	13.2_8	...$(R'S)(R'R)^{13}CH_3$	13.2_4
$^{13}CH_3(R'R)(R'S)$...	15.2_7	...$(R'R)(R'S)^{13}CH_3$	15.2_7
$^{13}CH_3(R'R)(R'R)$...	15.1_0	...$(R'S)(R'S)^{13}CH_3$	15.0_9

[a] The stereochemical environment of $^{13}CH_3$ is given by reporting on the right (for the "left" end groups) and on the left (for the "right" end groups) of $^{13}CH_3$ the configurations of the asymmetric carbons of the two first neighboring monomer units. Note that the position of $^{13}CH_3$ is not commutative. The configuration of the backbone asymmetric carbon of the monomer units is given according to the convention reported in note 21, i.e., considering the polymer chain still bound to the metal atom at the left end.

By definition this ratio is the diastereoselectivity of the propagation steps. Since the observed intensity ratio is $t/e \simeq 2.5$, it may be concluded that the diastereoselectivity of chain propagation is not much different from that of the initiation steps.

The complete assignment of the stereochemical structure of the observed "left" end groups can be achieved by comparing the chemical shifts of the $^{13}CH_3$'s with those observed for chemically equivalent $^{13}CH_3$'s on the "right" end groups (see Table VI). The assignment is in agreement with what is expected on the basis of the high enantioselectivity of the propagation steps and the employment of racemic monomer.

The other resonances shown in Figure 8 are those expected for the carbons of the inner monomer units. The resonances of the backbone methylene carbons are of course enhanced because of the selective ^{13}C enrichment of the monomer and appear to be spread between 29.5 and 32.5 ppm. The large spreading of these resonances as well as the maximum intensity observed at 30.4_4 ppm (very close to the chemical shift observed for the same carbon in isotactic poly[(*S*)-3MP1)] is qualitatively in agreement with the moderate degree of diastereoselectivity of the propagation.

Since a complete assignment of the chemical shifts observed for these CH_2 resonances as a function of the stereochemical environment is not available, a further check of the observed diastereoselectivity of the propagation is not possible at present.

3. Experimental Part

Reagents. ^{13}C-enriched (33%) $Al(^{13}CH_3)_3$ and $Zn(^{13}CH_3)_2$ were prepared and purified as previously described.[7a] (*RS*)-(1-^{13}C)3MP1 (45% enrichment) was prepared starting from enriched CH_3I and 2-methyl-1-butanal, with the modification of the Wittig reaction suggested by Greenwald and co-workers.[26] The enriched monomer was purified after distillation on $Al(C_2H_5)_3$: yield 70%. (*S*)-3MP1 was prepared according to a literature procedure;[27] $[\alpha]^{20}_D$ +32.9°. δ-$TiCl_3$ (HRA Stauffer) was purified by extraction with boiling toluene. (*S*)-3MP1 and (*RS*)-3MP1 (Fluka) were dried by distillation on $Al(CH_3)_3$.

Polymerization of (*RS*)-3MP1. To a suspension of δ-$TiCl_3$ (2 mmol) in 7 mL of toluene were added, with stirring, 4 mL of (*RS*)-3MP1, $Al(^{13}CH_3)_3$ (1.7 mmol), and $Zn(^{13}CH_3)_2$ (2.2 mmol) (33% enrichment).

The polymerization reaction was carried out at 50 °C for 3 days and then stopped with acidified methanol. The polymer (0.62 g), washed with pure methanol, was collected and dried under vacuum. The fractionation results are reported in Table I.

Polymerization of (*S*)-3MP1. The polymerization was carried out with (*S*)-3MP1 (4 mL), δ-$TiCl_3$ (3.2 mmol), $Al(^{13}CH_3)_3$ (1.7 mmol), and $Zn(^{13}CH_3)_2$ (1.4 mmol) (39% enrichment) in 7 mL of toluene. The polymerization time was 5 days at a temperature of 50 °C and the polymer yield was 1.25 g. The fractionation results are reported in Table II.

Polymerization of (*RS*)-(1-^{13}C)3MP1. Polymerization was performed at 50 °C by using δ-$TiCl_3$ (6.5 mmol), $Al(CH_3)_3$ (3.1 mmol), $Zn(CH_3)_2$ (3.6 mmol), anhydrous toluene (7 mL), and 45% enriched (*RS*)-(1-^{13}C)3MP1 (5 mL). Polymerization was stopped after 5 days; polymer yield: 0.09 g; cold methanol soluble fraction, ≃20%; boiling acetone soluble fraction, ≃25%; boiling toluene soluble fraction, ≃47%; boiling toluene unsoluble fraction, ≃8%.

Polymer Fractionation. Polymers were fractionated with boiling solvents by conventional methods.[28] The polymer fractions insoluble in boiling toluene were thermally degraded under high vacuum in order to obtain a soluble sample for the ^{13}C NMR analysis.

^{13}C NMR Analysis. ^{13}C NMR analysis of the polymer dissolved in 1,2,4-trichlorobenzene containing 1% HMDS as an internal standard was carried out at 140 °C in the PFT mode on a Bruker HX-90 spectrometer operating at 22.63 MHz. Pulse interval: 3.6 μs.

X-ray Analysis. X-ray spectra of unoriented samples were obtained with a Siemens D-500 X-ray spectrometer, using Cu Kα Ni-filtered radiation, a scan speed of 1 deg/min, a time constant of 1 s, a chart speed of 2 cm/min, and a window set of 0.3/0.3/0.3/0.018°.

4. Conclusion

By observing the stereochemical structure of isotactic poly[(*S*)-3MP1] and that of isotactic poly[(*RS*)-3MP1] we conclude that the *R'*,*R* and *S'*,*S* faces of the monomer are 2 times more reactive than the *R'*,*S* and *S'*,*R* faces in the considered initiation step.

The insertion of the chiral monomer into the Mt–CH_3 bonds performed on the chiral active sites of the Ziegler–Natta isotactic specific catalyst (initiation step) is diastereoselective to the same extent whatever the relative configuration of the chiral monomer and the active site.

The difference between the activation energies for the insertion of the favored monomer faces in comparison with the other ones (i.e., the diastereoselective driving force) can be estimated from the e/t ratio by means of the Arrhenius law $E_{R',R} - E_{R',S} \simeq 0.4$ kcal/mol.

The diastereoselective driving force seems essentially the same for the chain propagation steps. In fact, the ^{13}C NMR spectrum of isotactic poly[(*RS*)-3MP1] (see Figures 3 and 8) shows that the optical purity of the enantiomorphic macromolecules is not very high. On the other hand, the ^{13}C NMR spectrum of poly[(*S*)-3MP1] as well as the X-ray results show that the stereochemical sequence of the configurations of the backbone substituted carbons is highly isotactic. In order to account for this fact one has to assume that during propagation *R'*,*S* units are formed exclusively on the $C^*_{R'}$ sites and *S'*,*S* units on the $C^*_{S'}$ ones. This fact suggests that the driving force of the diastereoselectivity is almost negligible in comparison with enantioselective control.

Finally, it is quite likely that the stereochemical structure of the "left" end groups is representative of the diastereoselectivity of the chain propagation steps. Therefore, the experimentally observed stereochemical structure of the "left" end groups confirms once again that the propagation steps of isotactic polymerization of (*RS*)-3MP1 are diastereoselective to an extent comparable to that of the chain initiation on Mt–CH_3 bonds. The stereochemical sequence of the configurations of the chiral substituents of isotactic poly[(*RS*)-3MP1] is in at least qualitative agreement with this statement. Incorporation of 3MP1 does not match diastereoselective coordination on possible model compounds of the active sites.

Acknowledgment. Financial support of the Programma Finalizzato di Chimica Fine e Secondaria of the Italian

CNR is gratefully acknowledged.

References and Notes

(1) Natta, G.; Pino, P.; Mazzanti, G.; Corradini, P.; Giannini, U. *Rend. Acc. Naz. Lincei (VIII)* **1955**, *19*, 397. Such polymerization has been called "stereoselective" by Natta and Pino.
(2) Pino, P.; Ciardelli, F.; Montagnoli, G. *J. Polym. Sci., Part C* **1969**, *16*, 3256.
(3) Ciardelli, F.; Locatelli, P.; Marchetti, M.; Zambelli, A. *Makromol. Chem.* **1974**, *175*, 923.
(4) Pino, P. *Adv. Polym. Sci.* **1965**, *4*, 393.
(5) (a) Zambelli, A. *NMR Basic Princ. Prog.* **1971**, *4*, 101. (b) Zambelli, A.; Gatti, G.; Sacchi, M. C.; Crain, W. O.; Roberts, J. D. *Macromolecules* **1971**, *4*, 475. In this paper the word enantioselective is always related to carbon 2 (enantiotopic) of the monomer, which becomes chiral after the insertion. The word diastereoselective is used with reference to the different reactivity of the diastereotopic faces of the monomer toward the insertion.
(6) Shelden, R. A.; Fueno, T.; Tsunetsugu, T.; Furokawa, J. *J. Polym. Sci., Part B* **1965**, *3*, 23.
(7) (a) Zambelli, A.; Sacchi, M. C.; Locatelli, P.; Zannoni, G. *Macromolecules* **1982**, *15*, 211. (b) Zambelli, A.; Locatelli, P.; Sacchi, M. C.; Tritto, I. *Macromolecules* **1982**, *15*, 831.
(8) Wolfsgruber, C.; Zannoni, G.; Rigamonti, E.; Zambelli, A. *Makromol. Chem.* **1975**, *176*, 2765.
(9) Stereochemical notation proposed by: Frisch, H. L.; Malllows, C. L.; Bovey, F. A. *J. Chem. Phys.* **1966**, *45*, 1565.
(10) Grant, D. M.; Paul, E. G. *J. Am. Chem. Soc.* **1964**, *86*, 2984.
(11) The configurational notation is that of: Cahn, R. S.; Ingold, C. R.; Prelog, V. *Angew. Chem., Int. Ed. Engl.* **1956**, *5*, 365.
(12) Eight more stereochemical environments are possible. Since they are mirror images of the ones considered, they are omitted.
(13) As reported in a previous paper,[14] the vicinal methyl carbons lying on the same side of the Fisher projection are defined as erythro (e) and those lying on the opposite side are defined as threo.
(14) Zambelli, A.; Gatti, G. *Macromolecules* **1978**, *11*, 485.
(15) Lazzaroni, R.; Salvadori, P.; Bertucci, C.; Veracini, C. A. *J. Organomet. Chem.* **1976**, *99*, 475.
(16) Lazzaroni, R.; Salvadori, P.; Pino, P. *J. Organomet. Chem.* **1972**, *43*, 233.
(17) Unpublished results from our laboratory.
(18) The molecular weight of the polymer is very low due to the presence of $Zn(CH_3)_2$, which is an effective chain-transfer agent. The solubility of the polymer arises from the low molecular weight of the fraction (see Table II) and not from lack of stereoregularity. See, e.g.: Natta, G.; Giacchetti, E.; Pasquon, I.; Pajaro, G. *Chim. Ind. (Milan)* **1960**, *42*, 1091.
(19) Nozakura, S.; Takeuchi, S.; Yuki, H.; Murahashi, S. *Bull. Chem. Soc. Jpn.* **1961**, *34*, 1673.
(20) Petraccone, V.; Ganis, P.; Corradini, P.; Montagnoli, G. *Eur. Polym. J.* **1972**, *8*, 99.
(21) $C^*_{R'}$ are the chiral active sites preferring during the propagation (or even in the initiation if the alkyl group bonded to the active metal is primary and larger than CH_3) the addition of the monomer (either *R* or *S*) to give a backbone substituted carbon of *R'* configuration. On the $C^*_{S'}$ sites the mirror image steps occur, giving mirror image end groups. The configuration of the backbone substituted carbons is assigned as reported in the caption of Figure 4, i.e., neglecting the isotopic substitution and assuming that the left side of the growing chain has a higher rank since the active metal of the catalytic sites is assumed to be at the left side of the chain. A consequence of this convention is that the attack on the *R'* (or *S'*) face of the monomer gives *S'* (or *R'*) (see Figure 2) backbone substituted carbons. In the equations of Scheme I are reported the configurational notations of the monomer units. The configuration of the backbone carbons is primed. The drawing of the stereochemical environment of the end groups is reported in Figure 1 under the corresponding labeling (AI, etc.). The A-labeled end groups have the enriched $^{13}CH_3$ in an erythro relationship with the CH_3 of the substituent of the first inserted monomer unit and the B-labeled end groups have the $^{13}CH_3$ in a threo relationship.
(22) It is assumed that the propagation rate constants are the same as those reported in Schemes I and II for the insertion of the second monomer unit.
(23) No fraction showed $I_{BI}/I_{BIV} < 1$. Most probably this is due to the fact that the lowest molecular weight fraction (oligomer) is lost because of the solubility in methanol.
(24) Zambelli, A.; Locatelli, P.; Rigamonti, E. *Macromolecules* **1979**, *12*, 156.
(25) The equation is referred to the propagation steps on the *R'*-preferring sites. For symmetry the diastereoselectivity on the *S'*-preferring sites is the same:

$$\frac{k_{R'(R'S)(R'S)} + k_{R'(R'R)(R'S)}}{k_{R'(R'R)(R'R)} + k_{R'(R'S)(R'R)}} = \frac{k_{S'(S'R)} + k_{S'(S'S)(S'R)}}{k_{S'(S'S)(S'S)} + k_{S'(S'R)(S'S)}}$$

(26) Greenwald, H.; Chaykovsky, M.; Corey, E. J. *J. Org. Chem.* **1963**, *28*, 1128.
(27) Pino, P.; Lardicci, L.; Centoni, C. *J. Org. Chem.* **1959**, *24*, 1399.
(28) Natta, G.; Morandi, M.; Crespi, G.; Moraglio, G. *Chim. Ind. (Milan)* **1957**, *39*, 275.

A Computer Model for the Gel Effect in Free-Radical Polymerization

Wen Yen Chiu, Gregory M. Carratt, and David S. Soong*

Department of Chemical Engineering, University of California, Berkeley, Berkeley, California 94720. *Received July 1, 1982*

ABSTRACT: A mathematical model is developed to describe free-radical polymerization reactions exhibiting a strong gel effect. Diffusion limitation is viewed as an integral part of the chain termination process from the very beginning of polymerization. Its effect on the overall rate of termination gradually increases with conversion and becomes dominant around certain conversion levels traditionally associated with the onset of the gel effect. Influence of temperature, concentration, and molecular weight on the relative importance of reaction vs. diffusion is properly accounted for by the model. The model also considers the glass effect, which occurs only at very high conversions when even monomer diffusion to reactive radical sites is severely curtailed. Thus, the developed model describes the polymerization process over the entire course of reaction. Model predictions have been compared with literature data on conversion history and product molecular weights for isothermal poly(methyl methacrylate) polymerization.

Introduction

The two major sources of problems encountered in industrial liquid-phase polymerization processes are the heat released by the highly exothermic reactions and the great increase in viscosity of the reacting media over the course of polymerization. For a typical addition polymerization the heat of polymerization ranges from 10 to 20 kcal/mol, which can result in an adiabatic temperature rise of 200–400 °C. This large generation of heat, coupled with the low thermal diffusivity of the reacting mixture, often

0024-9297/83/2216-0348$01.50/0